Inorg. Chem. **2007**, *46*, 6871–6879

Gadolinium Acetylacetonate Tetraphenyl Monoporphyrinate Complex and Some of Its Derivatives: EXAFS Study and Molecular Dynamics Simulation

J. H. Agondanou,[†] I. Nicolis,[†,§] E. Curis,[†,§] J. Purans,[‡] G. A. Spyroulias,[||,⊥] A. G. Coutsolelos,*[,||] and S. Bénazeth*[,†,§]

Laboratoire de biomathématiques, Faculté de pharmacie, Université Paris Descartes, 75006 Paris, France, Institute of Solid State Physics, University of Latvia−Kengaraga 8, 1063 Riga, Latvia, L.U.R.E., Bat 209D, Université Paris XI, 91405 Orsay, France, and Laboratory of Bioinorganic Coordination Chemistry, University of Crete, Voutes Campus, 71003 Heraklion, Crete, Greece

Received September 28, 2006

Many attempts to obtain single crystals appropriate for X-ray diffraction analysis of the Ln(tpp)(acac) derivatives (where Ln = Gd or Sm, tpp = tetraphenylporphyrin and acac = acetylacetonate) have failed so far. A suitable way to get structural parameters for these monoporphyrinates is to use extended X-ray absorption fine structure (EXAFS) spectroscopy. We recorded spectra of the monoporphyrins, Ln(tpp)(acac) and Gd(tpyp)(acac) (where tpyp = tetrapyridylporphyrin), and the bisporphyrin GdH(tpyp)$_2$ in the solid state. We particularly focused our structural analysis on Gd(tpp)(acac), applying both molecular modeling and EXAFS, which allowed us to get accurate results about the local environment of the central atom. The Gd^{3+} ion of the complex at room temperature was found to be bonded to four monoporphyrin nitrogen atoms at an average distance $R(Gd–N_{av}) = 2.48$ Å and to three or four oxygen atoms at $R(Gd–O_{ac,w}) = 2.38$ Å from an acetylacetonato anion and a water molecule. The presence of the second water molecule in the coordination sphere was barely discernible by EXAFS analysis. Molecular modeling has provided further information about the coordination core geometry of the Gd(tpp)(acac) monoporphyrinate, including a bishydrated coordination sphere. Also, it has enabled the construction of a 3D structural model on which multiple scattering analyses were attempted. Monte Carlo simulation was used to validate the adjustments. EXAFS spectra analysis was carried out on the derivatives, displaying slight distortions in the lanthanide central-atom coordination geometry.

Introduction

The monoporphyrinate complex Ln(porphyrinate)(acac) (where Ln = Gd or Sm and acac = acetylacetonate) is essentially the precursor to the synthesis of many asymmetric double or triple deckers of strong importance and use in chemical and biological processes.[1−5] Considerable attention and intense interdisciplinary research are devoted to tetrapyrrolic macrocycles because they play a major biological role in molecular binding, catalysis, and electron and energy transfers.[6−11]

* To whom correspondence should be addressed. Phone: +30.2810.545045. Fax: +30.2810.545001. E-mail: coutsole@chemistry.uoc.gr.
[†] Université Paris Descartes.
[‡] University of Latvia−Kengaraga.
[§] LURE.
[||] University of Crete.
[⊥] Current address: Department of Pharmacy, University of Patras, 26500 Patras, Greece.

(1) Hoffman, B. M.; Ibers, J. A. *Acc. Chem. Res.* **1983**, *16*, 21.
(2) (a) Tsukube, H.; Shinoda, S. *Chem. Rev.* **2002**, *102*, 2389. (b) Schramm, C. J.; Scaringe, R. P.; Stojakovic, D. J.; Hoffman, B. M.; Ibers, J. A.; Marks, T. *J. Am. Chem. Soc.* **1980**, *102*, 6702.
(3) Deisenhofer, J.; Michel, H. *Science* **1989**, *245*, 1463.
(4) (a) Buchler, J. W.; Scharbert, B. *J. Am. Chem. Soc.* **1988**, *110*, 4272. (b) Buchler, J. W. *Comments Inorg. Chem. Soc.* **1987**, *112*, 3313.
(5) (a) Horrocks, W. D., Jr.; Wong, C. P. *J. Am. Chem. Soc.* **1976**, *98*, 7157. (b) Horrocks, W. D., Jr.; Venteicher, R. F.; Spilburg, C. A.; Vallee, B. L. *Biochem. Biophys. Res. Commun.* **1975**, *64*, 317. (c) Adler, A. D.; Longo, F. R.; Kampus, F.; Kim, J. *J. Inorg. Nucl. Chem.* **1967**, *32*, 476.
(6) (a) Burrell, A. K.; Officer, D. L. *Synlett.* **1998**, *25*, 1297. (b) Waluk, J. *J. Phys. Chem.* **1998**, *102*, 9999. (c) Segrestaa, J.; Vérité, P.; Estour, F.; Ménager, S.; Lafont, O. *Chem. Pharm. Bull.* **2002**, *50*, 744.
(7) (a) Perng, J. H.; Duchowski, J. K.; Bocian, D. F. *J. Phys. Chem.* **1990**, *94*, 6684. (b) Perng, J. H.; Duchowski, J. K.; Bocian, D. F. *J. Phys. Chem.* **1991**, *95*, 1319.
(8) (a) Tran-Thi, T. H.; Mattioli, T. A.; Chabach, D.; De Cian, A.; Weiss, R. *J. Phys. Chem.* **1994**, *98*, 8279. (b) Buchler, J. W.; Hammerschmitt, P.; Kaufeld, I.; Löffler, J. *Chem. Ber.* **1991**, *124*, 2151.

10.1021/ic061861x CCC: $37.00
Published on Web 07/21/2007

A large number of experimental papers was published on rare earth porphyrins in the last years,[12−18] based on XRD data for symmetrical or asymmetrical dimers like $Eu^{III}(oep)_2$, $Ce^{IV}(oep)(tpp)$, $Gd^{III}H(oep)(tpp)$, and $Sm^{III}H(oep)(tpp)$ (where tpp = tetraphenylporphyrin and oep = octaethylporphyrin).[19−22] However, there is a lack of structural data for monomeric species and the first X-ray crystal structure of a lanthanide(III) monoporphyrinic complex was determined only in 1997 by Coutsolelos et al., on a terbium compound $[Tb^{III}(\beta\text{-}Cl_8tpp)(O_2CMe)(Me_2SO)_2]$.[23] Nonetheless, in the case of the monoporphyrinates Gd(tpp)(acac) and Sm(tpp)(acac), only the lattice parameters have been obtained and XRD analysis by Jiang et al. for the detailed structure has not provided a complete characterization.[24]

The coordination geometry of Ln(III) monoporphyrinates has raised a lot of questions concerning the existence of a bonding between the metal and two water molecules. Yet, much was unknown about Ln(tpp)(acac) monoporphyrinates because they were inter alia formulated as hexacoordinated species.[5a,11] Actually, the mass spectra of those monoporphyrins did not show, in all the cases, the presence of the neutral ligand H_2O. Buchler et al.[25] suggested however that these complexes should be regarded as octacoordinated species $Ln(tpp)(acac)(H_2O)_2$, in view of the size of the lanthanide ions and by analogy to crystal structure determinations of rare earth monophthalocyaninates.[26] Furthermore, some measurements with infrared spectroscopy and XRD on other Ln monoporphyrins and phtalocyanines are in agreement with an octacoordination for this type of complex.[26,27] Hence, it appears that the question of the number of coordination for these rare earth elements is still open.

In this paper, we present an extended X-ray absorption fine structure (EXAFS) study for the Gd(tpp)(acac) complex, combined with molecular mechanics/molecular dynamics (MM/MD) modeling to obtain consistent local structural information. EXAFS spectroscopy was chosen because it is a powerful tool that provides direct structural information on cluster core geometry in any state up to 5 Å, while molecular modeling enabled the construction of a 3D model to examine the contribution in the spectra of the multiple scattering long paths. As we have underlined above, only one monomeric crystal structure is available,[23] and it is not suitable as a model because it concerns a Tb complex with ligands different from the ones of our compound. Such a crossed approach combining EXAFS spectroscopy and molecular modeling is not so frequently used because of the time needed, but it has been recently successfully applied to metalloproteins for near-edge structural studies.[28]

In this work, derivative complexes of Gd(tpp)(acac) were also studied to investigate if the structures are conserved when the metal is changed (comparison between Gd(tpp)(acac) and Sm(tpp)(acac) or when the ligand is changed, tpp being replaced by tpyp (tetrapyridylporphyrin), keeping or not the acac ligand. The results on the selected monoporphyrinates may help to understand the differences on the redox properties and the arising $\pi-\pi$ interactions in the corresponding bisporphyrinates (see Figure 1, the schematic diagram of the various ligands interacting with the lanthanide metals).

Experimental Section

Synthesis. All the lanthanide monoporphyrinate complexes have been synthesized from procedures well established by Wong et al.[11] The free base $(porph)H_2$ (with porph = tpp or tpyp) was synthesized according to the literature method,[5a,c] and 1,2,4-trichlorobenzene was purchased from Aldrich.

The synthetic route for monomeric species allowed us to achieve the synthesis of analogous hydrophilic complexes or the preparation of homo- and heteroleptic double deckers by direct reaction of the monoporphyrinates with in situ-prepared dilithium octaethylporphyrinate $Li_2(oep)$.[19] Actually, we have also synthesized a hydrogen bis[5,10,15,20-tetrakis-(4-pyridyl)porphyrinato] gadolinium(III), $GdH(tpyp)_2$.[13,22]

EXAFS Measurements. The microcrystalline powders of Gd(III) and Sm(III) derivatives mixed with cellulose were finely ground and pressed into a pellet at 10 tons of pressure. The homogeneous and 1 mm thick pastilles (to avoid saturation effects and reach the value of the absorption jump between 0.5 and 1) were held into a cardboard spacer with Kapton tape windows. Related to the low aqueous solubility of the complexes, we could not record the solution spectra which would have given too noisy data.

(9) (a) Harrison, B. S.; Foley, T. J.; Bouguettaya, M.; Boncella, J. M.; Reynolds, J. R.; Schanze, K. S.; Joonbo, S.; Holloway, P. H.; Padmanaban, G.; Ramakrishnan, S. *Appl. Phys. Lett.* **2001**, *79*, 3770. (b) Collman, J. P.; Kendall, J. L.; Chen, J. L.; Collins, K. A.; Marchon, J. C. *Inorg. Chem.* **2000**, *39*, 1661.

(10) (a) Horrocks, W. D., Jr.; Hove, E. G. *J. Am. Chem. Soc.* **1978**, *100*, 4386. (b) Chen, D.; Squattrito, P. J.; Martell, A. E.; Clearfield, A. *Inorg. Chem.* **1990**, *29*, 4368.

(11) Wong, C. P.; Venteicher, R. F.; Horrocks, W. D., Jr. *J. Am. Chem. Soc.* **1974**, *96*, 7149.

(12) (a) Duchowski, J. K.; Bocian, D. F. *Inorg. Chem.* **1990**, *29*, 4158. (b) Duchowski, J. K.; Bocian, D. F. *J. Am. Chem. Soc.* **1990**, *112*, 3313.

(13) Spyroulias, G. A.; Sioubara, M. P.; Coutsolelos, A. G. *Polyhedron* **1995**, *14*, 3563.

(14) Garcia-Sanchez, M. A.; Campero, A. *J. Non-Cryst. Solids* **2001**, *296*, 50.

(15) (a) Ng, D. K. P.; Jiang, J. *Chem. Soc. Rev.* **1997**, *26*, 433. (b) Jiang, J.; Machida, K. I.; Yamamoto, E.; Adachi, G. Y. *Chem. Lett.* **1991**, 2035.

(16) Gross, T.; Chevalier, F.; Lindsey, J. S. *Inorg. Chem.* **2001**, *40*, 4762.

(17) Campazzi, E.; Solari, E.; Scopelliti, R.; Floriani, C. *Inorg. Chem.* **1999**, *38*, 6240.

(18) Wong, W. K.; Zhang, L.; Wong, W. T.; Xue, F.; Mak, T. C. W. *J. Chem. Soc., Dalton Trans.* **1999**, 615.

(19) Buchler, J. W.; De Cian, A.; Fischer, J.; Kihn-Botulinski, M.; Weiss, R. *Inorg. Chem.* **1988**, *27*, 339.

(20) Buchler, J. W.; De Cian, A.; Fischer, J.; Hammerschmitt, P.; Löffler, J.; Scharbert, B.; Weiss, R. *Chem. Ber.* **1989**, *122*, 2219.

(21) Spyroulias, G. A.; Raptopoulou, C. P.; De Montauzon, D.; Mari, A.; Poilblanc, R.; Terzis, A.; Coutsolelos, A. G. *Inorg. Chem.* **1999**, *38*, 1683.

(22) Spyroulias, G. A.; Coutsolelos, A. G.; Raptopoulou, C. P.; Terzis, A. *Inorg. Chem.* **1995**, *34*, 2476.

(23) Spyroulias, G. A.; Despotopoulos, A.; Raptopoulou, C. P.; Terzis, A.; Coutsolelos, A. G. *Chem. Commun.* **1997**, 783.

(24) Jiang, J.; Hu, T. D.; Xie, J. L.; Li, C.; Zhang, J. Z. *Chin. J. Chem.* **1998**, *16*, 425.

(25) Buchler, J. W.; De Cian, A.; Fischer, J.; Kihn-Botulinski, M.; Paulus, H.; Weiss, R. *J. Am. Chem. Soc.* **1986**, *108*, 3652.

(26) De Cian, A.; Moussavi, M.; Fischer, J.; Weiss, R. *Inorg. Chem.* **1985**, *24*, 3162.

(27) Buchler, J. W.; De Cian, A.; Fischer, J.; Kihn-Botulinski, M.; Paulus, H.; Weiss, R. *J. Am. Chem. Soc.* **1986**, *108*, 3652.

(28) Chan, J.; Merrifield, M. E.; Soldatov, A. V.; Stillman, M. A. *Inorg. Chem.* **2005**, *44*, 4923.

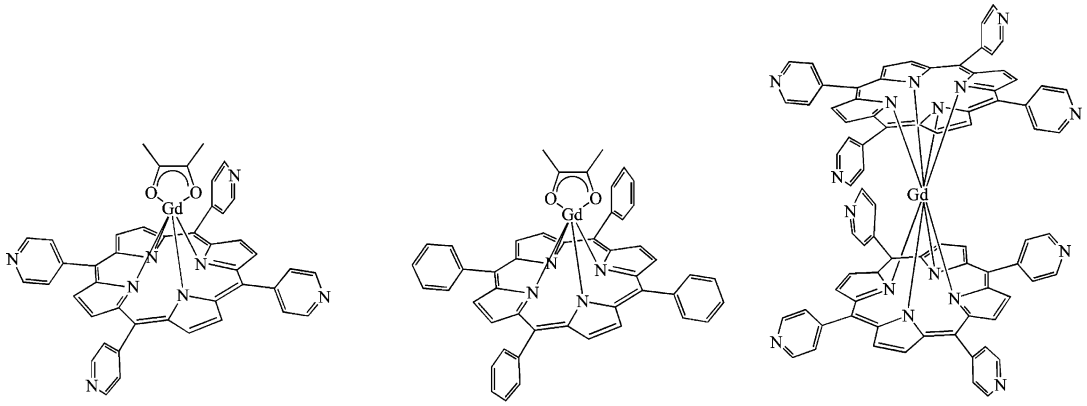

Figure 1. Schematic diagrams of the (acac), (tpp), and (tpyp) ligands interacting with lanthanide Ln metal ions. For the porphyrinic ligand, the carbon atoms of the pyrroles are labeled C_α, C_β, and C_γ for the meso atoms and $C_{\phi 1}$ for the first carbon of the phenyl or pyridyl groups. For the acac ligand, the oxygen atoms are labeled O_{acac}, and the carboxylate carbon atoms C_{acac}.

X-ray absorption measurements were performed for all samples at the LURE-DCI storage ring (Orsay, France) on XAS 2 and XAS 13 beam line stations with positron beam energy of 1.85 GeV and mean current of 300 mA. The spectrometers were equipped with a double-crystal monochromator using air-filled ionization chambers for transmission measurements and a solid-state Canberra germanium 7-element array detector for fluorescence measurements. Internal energy calibration was performed at the Fe K edge (7147 eV) close to the Gd L_3 edge (7241 eV), and harmonic rejection was achieved by slightly detuning the parallelism of the crystals to 30% of the maximal intensity.

To decrease an excessive influence of the Debye Waller (DW) factor and reduce the thermal agitation and damping effects on the EXAFS signal, the samples were cooled in liquid nitrogen and kept at 80 K throughout storage and data collection.

The Gd L_3 edge spectra were recorded in transmission mode at room and low temperatures (RT and LT, respectively) for the Gd(tpp)(acac) complex with a Si(311) double-crystal monochromator (XAS 13 station), whereas for the Gd complexes with tpyp ligands, data were collected both in transmission mode and fluorescence only at room temperature (RT) with a Si(111) monochromator increasing the reflected beam intensity with the drawback of a loss of resolution (XAS 2 station).

For the lipophilic Gd(tpyp)(acac), six spectra were collected in transmission mode with a 1 eV step, a 2 s per point count time, and an energy scan from 7100 to 7900 eV, but the data were truncated at 7750 eV because of the signal-to-noise level. Five spectra were recorded in fluorescence mode, with a 1 eV step and a 10 s per point count time. For fluorescence measurements, we had to reduce by 1/3 the mass of sample to avoid self-absorption effects. The fluorescence technique is known to be more sensitive than transmission, especially for the study of dilute systems or low concentrated samples, but the quantitative information accessible via these two modes of recording remains identical.

For the Sm derivative, the measurements were performed in transmission mode at RT with a Si(111) crystal monochromator. The range of the L_3 edge (E_{L3} = 6716 eV) EXAFS is limited by the presence of the Sm L_2 edge (E_{L2} = 7320 eV). Therefore the experimental spectra were collected in the energy range from 6600 to 7300 eV with a step of 1 eV, count rate of 2 s per point, and energy resolution (fwhm) of 2.0 eV. The slit width was studied and adjusted to render the spectra well defined for the data analysis.

EXAFS Data Analysis. The EXAFS oscillations were extracted using standard techniques and refinement procedures.[29] The experimental data were analyzed with the LASE program, providing new tools for statistical error evaluation of the refined parameters.[30] The background contribution was estimated by a Victoreen-like function and subtracted from the experimental spectrum, whereas the atomic-like contribution was calculated by a combined polynomial/cubic-spline technique to have a precise removal of the EXAFS signal baseline.[31,32] For all the complexes, the EXAFS signal $\chi(k)$ was k^2 weighted to enhance the impact of high k data because of the decay of the photoelectron wave (k^3 weighting gave too noisy data).

Calculations of the EXAFS function were performed for the first coordination sphere, based on the single-scattering (SS) curved-wave formalism. By fitting on the filtered first peak of the FT transform, it was impossible to distinguish between models accounting for one or two water molecules. Previous calculations had shown that multiple scattering (MS) effects would appear beyond the first coordination sphere in porphyrinic complexes.[33] Therefore, we decided to fit the unfiltered data and to include MS effects.

To reach this aim, we needed a 3D structural model, which we obtained by molecular dynamics simulations. All the

(29) (a) Co, M. C.; Hodgson, K. O. *J. Am. Chem. Soc.* **1981**, *103*, 3200. (b) Jalilehvand, F.; Lim, B. S.; Holm, R. H.; Hedman, B.; Hodgson, K. O. *Inorg. Chem.* **2003**, *42*, 5531.
(30) (a) Curis, E.; Bénazeth, S. *J. Synchrotron Radiat.* **2000**, *7*, 262. (b) http://www.esrf.fr/computing/scientific/exafs/lase.html.
(31) (a) Rocca, F.; Kuzmin, A.; Purans, J.; Mariotto, G. *Phys. Rev.* **1994**, *B50*, 6662. (b) Kuzmin, A.; Purans, J.; Benfatto, M.; Natoli, C. R. *Phys. Rev.* **1993**, *B47*, 2480.
(32) Agondanou, J. H.; Spyroulias, G. A.; Purans, J.; Tsikalas, G.; Souleau, C.; Coutsolelos, A. G.; Bénazeth, S. *Inorg. Chem.* **2001**, *40*, 6088.
(33) Poncet, J. L.; Guilard, R.; Friant, P.; Goulon-Ginet, C.; Goulon, J. *New J. Chem.* **1984**, *8*, 583.

ligation shells that have been shown to contribute to the overall signal were used to simulate EXAFS spectra for the Gd metal with the ab initio FEFF (7.02 version)[34] program. The calculations are based on self-consistent final-state potentials. The scattering potential is approximated by overlapped spherical muffin-tin potential (including a core hole, $\Gamma_{core-hole} = 3.5$ eV for $2p_{3/2}$ level in the case of the Gd L_3 edge). Many body effects are incorporated approximately in terms of a complex, energy-dependent self-energy. The Dirac−Hara energy-dependent potential was used with the addition of the photoelectron mean-free path contribution automatically included in the scattering amplitude function using the complex Hedin−Lundqvist exchange.[35]

Monte Carlo Statistical Errors Analysis. Once the model was built up and validated, a new goal was to estimate the uncertainties on the fitted parameters. Mainly three methods are proposed in the literature, but the Monte Carlo error analysis method is the most appropriate when the experimental distribution model is known.[36,37] Here, as the data collection was repeated at least 5 times, this Monte Carlo simulation can be used, generating 1000 pseudo-experimental spectra following a Gaussian distribution, and using the experimental error bars determined. The detail of the procedure has already been published,[38] and the estimated errors correspond to the statistical uncertainty. However, the values obtained did not include systematic errors that cannot be estimated by any of the methods. By this procedure, we obtained not only average values and errors but also the complete population distribution of the different solutions, especially informative in cases of multimodal solutions resulting from numerical instability.

Molecular Dynamics Simulations. Molecular dynamics simulations were performed using the parallel 3.1.4 version of the GROMACS package,[39,40] on a dual processor Athlon computer, under a Linux operating system. The OPLS (optimized potentials for liquid simulations) all-atom force field[41,42] includes rare-earth parameters[43] and was used for all calculations. Here, arises the question of comparing EXAFS solid-state spectra and MM/MD calculations operated in solution. We have assumed that, relative to the structural rigidity of the tpp and acac ligands, their geometry will be conserved in both states. Furthermore, it has been shown in earlier studies[44,45,46] that the local environments of the Gd^{3+} center are greatly similar in solution and in the solid state.

A constant temperature of 300 K and pressure of 1 bar were applied by coupling to an external bath.[47] Particle-mesh Ewald was used for long-range electrostatics with a 1.4 nm direct space cutoff, and long-range dispersion corrections were applied for energy and pressure.

An OPLS methanol (to take into account the very low aqueous solubility of the complex) periodic cubic box was built with a 5 nm edge length and allowed to equilibrate until constant density was reached. Tetraphenylporphyrin and acetylacetonate models were also built with standard OPLS parameters except that Wang−Ford partial charges were computed by Mopac software at the AM1 (Austin Model 1) level of theory. The tetraphenylporphyrin and the acetylacetonate molecules were placed together with a Gd^{3+} atom in a periodic cubic box of 5 nm edge, and solvated first with 90 TIP3 water molecules at random positions and then with 1690 methanol molecules from the above-mentioned equilibrated methanol box. A first constrained dynamics run allowed the system to relax to remove bad contacts, followed by unconstrained equilibration run of 2 ns and a production run of 6 ns, with steps of 1 fs.

The force field was further calibrated and adjusted through comparison between experimental spectra and simulated EXAFS spectra calculated using the FEFF program in combination with atomic coordinates from MM/MD energy minimization. Through the comparison between experimental and calculated EXAFS data, the coordination environment that best matches the metal binding site can be identified.[28]

Results and Discussion

Gd(tpp)(acac) Complex. Among all the compounds reported here, we studied extensively the Gd(tpp)(acac) complex. The detailed structural analysis performed on this complex will serve as reference for the investigation of the other derivatives.

The experimental EXAFS spectra at room and low temperatures are presented in Figure 2a. Sharp multielectron resonances above the L_3 edge of Gd^{3+} ion are observed with the presence of anomalous peak at about 6 $Å^{-1}$. But, the distortion in the experimental EXAFS structural oscillations is very low and moreover the contribution of this double-excitation is beyond the region of interest at about 5 Å.

The magnitude of the non-phase-shift-corrected Fourier transforms (FTs) of the EXAFS spectra for Gd(tpp)acac complex is displayed in Figure 2b. The FT is composed of one main peak labeled A and a series of lower peaks from 2.6 to 4.5 Å. The low intensity of the FT signal above 5.5 Å indicates that the noise in the experimental spectrum has a

(34) (a) Rehr, J. J.; Mustre de Leon, J.; Zabinsky, S. I.; Albers, R. C. *J. Am. Chem. Soc.* **1991**, *113*, 5135. (b) Zabinsky, S. I.; Rehr, J. J.; Ankudinov, A.; Albers, R. C.; Eller, M. J. *Phys. Rev.* **1995**, *B52*, 2995.
(35) Kuzmin, A.; Obst, S.; Purans, J. *J. Phys. Rev.: Condens. Matter* **1997**, *9*, 10065.
(36) *IXS Standard and Criteria Subcommittee Reports: Error Reporting Recommendations*; International XAFS Society: Camerino, Italy, 2000; http://ixs.iit.edu/subcommittee_reports/sc/index.html.
(37) Curis, E.; Bénazeth, S. *J. Synchrotron Rad.* **2005**, *12*, 361.
(38) Curis, E.; Bénazeth, S. *J. Synchrotron Rad.* **2001**, *8*, 264.
(39) Lindahl, E.; Hess, B.; van der Spoel, D. *J. Mol. Model.* **2001**, *7*, 306.
(40) Berendsen, H. J. C.; van der Spoel, D.; van Drunen, R. *Comp. Phys. Commun.* **1995**, *91*, 43.
(41) Jorgensen, W. L.; Maxwell, D. S.; Tirado-Rives, J. *J. Am. Chem. Soc.* **1996**, *118*, 11225.
(42) Kaminski, G. A.; Friesner, R. A.; Tirado-Rives, J.; Jorgensen, W. L. *J. Phys. Chem. B* **2001**, *105*, 6474.
(43) van Veggel, F. C. J. M.; Reinhoudt, D. N. *Chem.—Eur. J.* **1999**, *5*, 90.
(44) Dubost, J. P.; Léger, J. M.; Langlois, M. H.; Meyer, D.; Schaefer, M. *C. R. Acad. Sci. Ser II.* **1991**, *312*, 349.
(45) Bénazeth, S.; Purans, J.; Chalbot, M. C.; Nguyen-van-Duong, M. K.; Nicolas, L.; Keller, F.; Gaudemer, A. *Inorg. Chem.* **1998**, *37*, 3667.
(46) Moreau, J.; Guillon, E.; Pierrard, J. C.; Rimbault, J.; Port, M.; Aplincourt, M. *Chem.—Eur. J.* **2004**, *10*, 5218.
(47) Berendsen, H. J. C.; Postma, J. P. M.; DiNola, A.; Haak, J. R. *J. Chem. Phys.* **1984**, *81*, 3684.

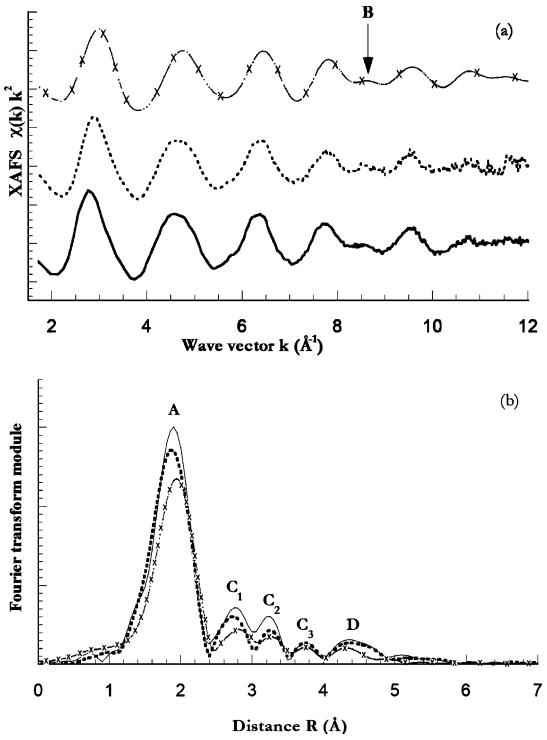

Figure 2. (a) XAFS spectra and (b) FTs (modulus part) of the Gd(tpp)(acac) complex at RT (dotted line) and LT (solid line) and simulated from the MM/MD calculations (crossed line). The spectral simulation from MM/MD model closely resembles the experimental data within noise, even for the scattering pattern (feature B) at $k = 8.5$ Å^{-1}.

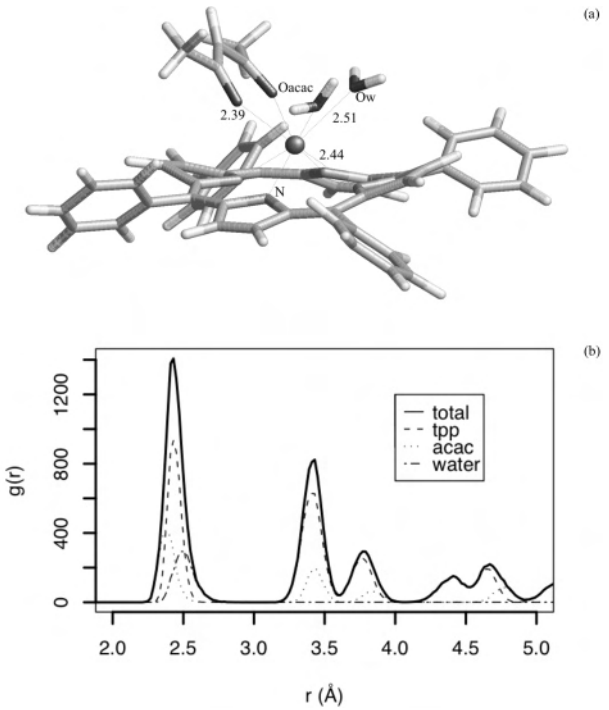

Figure 3. (a) Gd(tpp)(acac) complex scheme from molecular modeling (MD) with calculated average distances of the oxygen atoms from the acac ligand R(Gd−O$_{ac}$) = 2.390 ± 0.056 Å, from the two water molecules R(Gd−O$_w$) = 2.514 ± 0.076 Å, and the four tpp-nitrogen atoms R(Gd−N$_{av}$) = 2.441 ± 0.047 Å. (b) The reconstructed radial disribution function (RDF) from MD simulations. This RDF provides additional insight into all different ligation shells and structural parameters for the Gd(tpp)acac metal−coordination structure up to 5 Å.

"white" character. The absence of any significant contribution near $R = 1$ Å indicates a good removal of the μ_0 signal. In the major first peak, a sharper feature for the LT spectrum is observed in comparison to the one at RT, for which the magnitude of the further peaks decreases more rapidly being more sensitive to thermal disorder as expected.

Single-Scattering Approach. First, we focused on the first coordination sphere in a single-scattering approach via peak A inverse Fourier transform analysis. We wanted to distinguish the contribution of the nitrogen atoms belonging to the porphyrinic ring from the oxygen atoms of the acetylacetonato anion and water molecules. Therefore, we carried out various fitting procedures using the scattering amplitudes and phases calculated by FEFF7: (1) a one-shell fitting merging the nitrogen and oxygen neighboring atoms, (2) a two-shell fitting discriminating N and O with respect to their characteristic distances, and (3) a three-shell fitting where we tried to show the water molecule bonding.

We found that the use of the two-shell fit model (procedure 2) agreed fairly well with the experimental values for the Gd(tpp)(acac) complex, when considering seven or eight (four N at 2.46 Å and three or four O at 2.39 Å, two from the acac ligand and one or two from water ligands) atoms close to the Gd^{3+} ion. The fitting weighted residuals values are 0.022 and 0.018 for one or two water molecules, respectively. The resulting distances for the oxygen atoms are relatively close to the one found by Jiang et al.[24] However, the distance value obtained by Jiang et al.[24] for the nitrogen atoms shell ($R_{Gd-N} = 2.33$ Å) appears to be too small compared to our result. On the basis of our analysis and XRD data from a lutetium phtalocyaninate complex,[27] the expected distances Gd−N must be larger than for a Lu ion (mean value Lu−N = 2.34 Å) according to the ionic radii and the well-known lanthanide contraction effect.

Even if the residual is smaller for the two water molecule model, the difference is too small to accept this model without further evidence, which we present later in this paper. We assumed that the one or two water ligands are at longer distances than acac and more loosely bound. So the mean oxygen shell merging O_w and O_{acac} corresponds to a distribution with high DW factor. These phenomena are confirmed by the water molecule RDF, computed from the model of the dynamics simulation, for which the peak is strongly damped and rather broadened in comparison to the peak of the O_{acac} (Figure 3).

Molecular Dynamics Results. We built, by molecular dynamics simulation, a 3D model necessary to compute the MS. Molecular dynamics confirm that there is no steric hindrance for water coordination on the Gd^{3+} atom simultaneously to tpp and acac ligands. The number of the Gd^{3+} neighbors closer than 3 Å remains constant at eight over the 6 ns trajectory. The first coordination sphere is composed by the two acetylacetonate oxygen atoms at the shortest distance with a mean value of 2.39 ± 0.06 Å, the four tpp-nitrogen atoms at an average distance of 2.44 ± 0.05 Å, and two oxygen atoms from two water molecules at a mean distance of 2.51 ± 0.08 Å (Figure 3a). These Gd^{3+}−N and Gd^{3+}−O_{acac} average distances are similar to the ones found by EXAFS SS analysis. Two water molecules are found with

Table 1. Structural Data Obtained from the Best-Fit Analysis on the Raw Data of the Gd(tpp)(acac) Complex (RT), with a Monte Carlo Statistical Errors Analysis Taking into Account All SS and MS Paths

paths	N	R (Å)	σ^2 (Å^2)
path 1: Gd−N−Gd	4	2.38 ± 0.06	0.017 ± 0.016
path 2: Gd−O−Gd	4	2.48 ± 0.03	0.009 ± 0.006
path 3: Gd−C_α−Gd	4	3.40 ± 0.26	0.011 ± 0.004
path 4: Gd−O_{acac}−C_{acac}−Gd	4	3.59 ± 0.01	0.0002 ± 0.0003
path 5: Gd−C_β−Gd	8	4.42 ± 0.67	0.049 ± 0.007
path 6: Gd−C_β−N−Gd	16	4.68 ± 0.22	0.007 ± 0.01[a]
path 7: Gd−$C_{\Phi 1}$−Gd	4	5.26 ± 0.64	0.009 ± 0.04[a]

[a] For pathways 6 and 7, large uncertainties on the DW factor are found. Both pathways are necessary for the adjustment as they improve the fitting results, but their contribution to the signal is too weak to be determined with accuracy.

this MM/MD simulation but at a greater distance than the EXAFS SS analysis result, where no discrimination between O atoms from water or acac was possible. Discrepancies between experimental and modeled coordination numbers have previously been described and assigned to dilution and ion-pairing effects[43] or many body effects.[48] The tpp macrocycle presents distortions from planarity and the *meso*-phenyl groups are tilted from the tetrapyrroles plane, as observed in the Cambridge Structural Databank tpp structures (mean tilt computed from 1138 structures).

Multiple Scattering Approach. We used the 3D model from MM/MD to generate the MS paths. First, we checked that the model coordinates gave a calculated EXAFS close to the experimental one, except for the E_0 and Debye−Waller that we adjusted (Figure 2). The simulation model reproduces well the overall beat pattern of the Gd(tpp)(acac) data and especially the beat node at $k = 8.5$ Å^{-1} (feature B in Figure 2a).

Then, we carried out the calculations with a cluster of 34 atoms within a radius of 5 Å, taking into account all SS and MS paths up to 6.5 Å. We obtained 427 pathways (34 SS and 393 MS) that were combined by geometrical analogies (successive shells of identical atoms with a difference in distance up to 0.1 Å and in angle up to 20°). Thus, 83 groups of pathways out of the total 427 paths were obtained, for which only 68 paths gave a contribution higher than 4%, compared to the highest contribution of the shortest path Gd−O_{acac} and Gd−N.

After consistency checking and validation of the different paths with various fits, seven paths having the most preponderant contributions to the overall EXAFS signal are selected as listed in Table 1; their contributions are given in the Supporting Information in Figure S1. With those paths, we reached a good agreement between the simulated MM/MD model and the experimental raw data (see Figure 4).

For the first coordination sphere, the two Gd−N and Gd−O single-scattering paths contribute to the first peak (A) of the FT, with four oxygen atoms (two from acac and two from water molecules) and the four nitrogen atoms of the monoporphyrin at average distances of R(Gd−O) = 2.48 Å and R(Gd−N) = 2.38 Å respectively. The MS effects related only to atoms of this first coordination sphere (group of pathways of O−Gd−O, O−Gd−N, and N−Gd−N) give a broad signal in the FT (about 20 paths with $R = 3.63-4.49$ Å), leading to a very small contribution to the total EXAFS signal. Actually, no significant improvement of the fit was observed when these pathways were introduced, and they can be neglected.

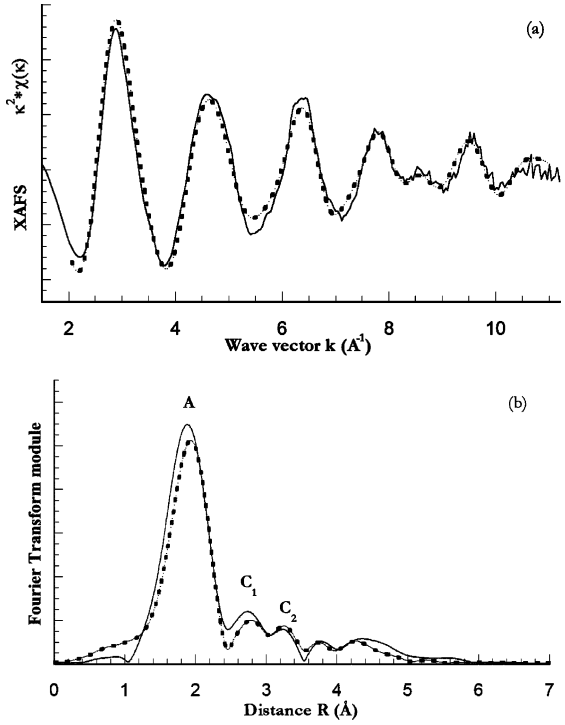

Figure 4. (a) Experimental (solid line) and least-squares fitted (dashed line) EXAFS raw data at RT of the Gd(tpp)(acac) complex and (b) the corresponding Fourier transforms.

The MS contribution is important for the outer coordination spheres. Indeed, only three single-scattering paths (Gd−C_α−Gd, Gd−C_β−Gd, and Gd−$C_{\Phi 1}$−Gd) contribute to this region, together with two MS paths (Table 1 and Figure S1). Other single-scattering paths, such as Gd−C_{acac}−Gd and Gd−C_γ−Gd, refine to very high DW factors and do not improve the fit, mainly, because of destructive interferences with the MS paths. For example, the double-scattering path Gd−O_{acac}−C_{acac}−Gd (which significantly improves the fit) has its frequency very close to the one of the Gd−C_{acac}−Gd (R = 3.60 Å) single-scattering path, and they both therefore contribute to the same region in R space. The two signals were found out-of-phase with similar amplitudes leading to a cancellation of the Gd−C_{acac}−Gd contribution. Such a cancellation interference effect has already been observed, especially for ions in solution EXAFS signals.[35] Such results are not in contradiction to the existence of carbon atoms in the coordination core geometry of the Gd metal but show that this second shell contribution can be strongly damped in EXAFS because of the cancellation interference effect with other multiple-scattering signals. The characteristic beat feature B in Figure 2a is the result of the interferences between the single paths Gd−C_α−Gd and Gd−C_β−Gd and the MS path Gd−N−C_β−Gd. Omission of any of these three paths leads to the fit failing to reproduce the beat pattern.

After the achievement of the fitting procedure, an estimation of the uncertainties has been made with a Monte Carlo

(48) Kerdcharoen, T.; Morokuma, K. *J. Chem. Phys.* **2003**, *118*, 8856.

statistical errors analysis. The estimated uncertainties on the structural parameters for Gd(tpp)(acac) are listed in Table 1. The Monte Carlo analysis permits us to take into account fitting instabilities on the distances and the Debye−Waller factors and understand them in terms of structural information as already exemplified.[37] In fact, we observe that the results are not unimodally distributed. On the contrary, different maxima are observed correlated between them. Thus, the average distances and Debye−Weller factors given in Table 1 are only apparent means, not necessarily reflecting the most probable solution. For example, the two paths of the first coordination sphere have their maximum probabilities located at 2.39 and 2.52 Å with Debye−Waller factors at 0.005 $Å^2$ and 0.014 $Å^2$ for N and O neighbors, respectively. We notice that in contrast to the apparent mean value, the major mode N atoms Debye−Waller factor is lower than the one of O atoms, as expected.

Other Derivatives. The other monoporphyrin derivatives were also studied with a fitting procedure on their raw data taking into account all single- and multiple-scattering paths calculated by FEFF with coordinate sets from MM/MD simulation on the Gd(tpp)(acac) complex. For the bisporphyrin $GdH(tpyp)_2$, various fits of the experimental data were performed with theoretical amplitudes and phases extracted from XRD data of the bisporphyrin GdH(oep)(tpp).

Sm(tpp)(acac) Complex. The experimental XAFS data of the Ln(tpp)(acac) compounds are globally similar, especially for k below 8 $Å^{-1}$ and in the major peak (A) of the FT. The model construction and adjustment encounters the same problems as for the Gd(tpp)(acac) complex. Application of analogous procedures yields similar results. For Sm(tpp)(acac), the fitting procedure has confirmed an octacoordination, with 4 nitrogen atoms at a mean distance of 2.48 ± 0.02 Å and 4 oxygen atoms (2 from acac, 2 from H_2O) at an average distance of 2.42 ± 0.02 Å (see Table S1). The Gd−O (2.39 Å) distance is slightly shorter than the Sm−O (2.42 Å) distance in agreement with an increase in the ionic radii. This trend is consistent with previous investigations made on Gd and Sm bisporphyrins.[32]

Gd(tpyp)(acac) Complex. The tetrapyridylporphyrin possesses almost the same structure as the tetraphenylporphyrin, except that it has nitrogen atoms instead of carbon in *para* position of the benzyl *meso*-substituents.

The EXAFS spectra and FTs of Gd(tpyp)(acac) and its analogue Gd(tpp)(acac) show small differences, the first FT peak of Gd(tpyp)(acac) being of higher magnitude and the further peaks being slightly shifted toward higher distances for Gd(tpyp)(acac).

The fitting procedure was performed using theoretical amplitudes and phases by FEFF with coordinate sets from the Gd(tpp)(acac) MM/MD simulation. During this fitting procedure, the coordination number for the nitrogen atoms was kept constant equal to 5 (considering the four nitrogen atoms of the pyrroles and one nitrogen atom belonging to a close pyridyl ligand from a neighboring macrocycle, according to a previous study).[49] The coordination number of oxygen atoms were kept equal to 3: two from the acac ligand and one from the water molecule (considering the steric hindrance of the pyridinic groups that precludes a second water molecule coordination). The adjustment interval varies from 2 to 11 $Å^{-1}$, with $N_{ind} = 10$ ($\Delta k = 9$ $Å^{-1}$ and FT windows width $\Delta R = 1.5$ Å). The structural parameters determined are gathered in the Table S1, following the two modes of EXAFS spectra recording: TM (transmission mode) and FM (fluorescence mode) for which we observed a perfect accordance. For the first coordination sphere of Gd(tpyp)(acac), an average Gd−N distance of 2.45 Å has been found, close to the Gd(tpp)(acac)'s one, but the difference between the two complexes is more marked when analyzing the second coordination sphere. For this step, we could not use the MS formalism because we did not perform time-consuming MM/MD calculations on this complex. By applying FT differences, we could describe the C_1 peak as a contribution of the eight C_α at 3.46 Å, which is slightly larger than for its analogue with tpp ligand (3.40 Å). These subtle differences between the two Gd monomers are correlated to the fact that for Gd(tpyp)(acac), the nitrogen atoms of the pyridyl group can coordinate to the central metal atom of another porphyrin molecule, playing thus the role of an axial ligand, stabilizing the reactive intermediate but modifying the structural environment of the Gd metal and resulting in a stretching of the macrocycle.[49] However, an alternative explanation for this lengthening could be the omission of an MS contribution as observed at 3.59 Å for the Gd(tpp)(acac) compound (Table 1).

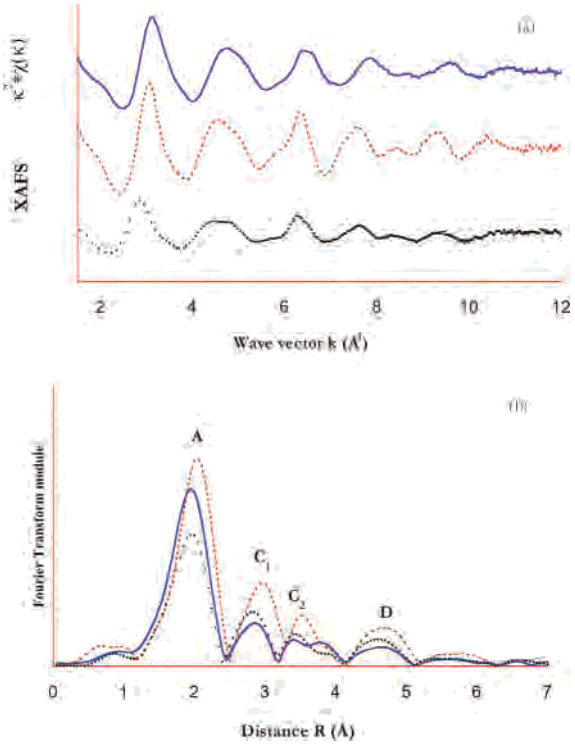

Figure 5. (a) Experimental EXAFS spectra and (b) Fourier transforms in transmission mode at RT of the monoporphyrin Gd(tpyp)(acac) (solid line) and bisporphyrins $GdH(tpyp)_2$ (dashed line) and $GdH(tpp)_2$ (dotted line).

$GdH(tpyp)_2$ Complex. The EXAFS spectra and FTs of Gd(tpyp)(acac), $GdH(tpyp)_2$, and $GdH(tpp)_2$ complexes are presented in Figure 5. We have noticed on these figures

(49) Davoras, E. M.; Coutsolelos, A. G. *J. Inorg. Biochem.* **2003**, *94*, 161.

important differences between the complexes confirmed by the fitting results (see Table S2).

The values found for the dimer $GdH(tpyp)_2$ correspond to a Gd photoabsorber, surrounded by eight nitrogen atoms at an average distance of 2.53 Å. This result differs significantly from the one obtained in our previous work[32] with the $GdH(tpp)_2$ complex, for which we had found an average distance of 2.45 Å for six nitrogen atoms and two other imine nitrogens with longer bonding effects resulting from their protonation at an average distance of 2.66 Å. The influence of the protonation on the first shell around the Gd central atom of the $GdH(tpyp)_2$ complex is not as strong as that for the $GdH(tpp)_2$ complex, and here, the symmetry is preserved. This is probably the result of a strong delocalization of the proton on all the nitrogen atoms of the macrocycle even the ones belonging to the pyridyl ligands or in the protonation of one pyridyl instead of a pyrrole nitrogen atom. No asymmetry of distribution of the distances was observed for the first coordination sphere of the $GdH(tpyp)_2$. In addition, no longer bonding effect caused by the protonation was observed, and so, the octacoordination is preserved.

The metal−carbon distances determined for the bisporphyrins for the second coordination sphere are very close. For $GdH(tpyp)_2$, an average distance $Gd-C_1$ of 3.48 Å has been found and attributed to sixteen C_α from the two cycles, very similar to that of its analogue $GdH(tpp)_2$ with a distance of 3.46 Å (see table S.2). There is also a slight difference in the $Gd-C_2$ distances between the values observed for the two bisporphyrinates (mean value 3.87 Å for tpyp and 3.78 Å for tpp). The differences between the bisporphyrinates are particularly acute for the first coordination sphere and obviously less pronounced for the second coordination sphere.

The electrochemical behavior of these gadolinium(III) porphyrin sandwichlike complexes has already been investigated, showing that the tpyp double-decker oxidizes considerably harder but reduces quite easily compared to the corresponding tpp double-decker.[50] This reflects the fact that thermodynamic basicities of porphyrins can be correlated to their structural parameters. Actually, the tpyp bisporphyrinate exhibits an extended π conjugation, which causes delocalization of the core electron density, thus decreasing the intrinsic basicity of the macrocycle.[51] The tpyp-complex exhibits therefore more symmetrical distribution of distances by EXAFS analysis than its tpp analogue. Moreover the longer coordination distance we found for tpyp compared to tpp is in accordance with the tpyp lower basicity. We have evidenced here the correlation between purely structural factors and electronic ones.

Conclusions

This work has afforded the elucidation of the metal−binding Ln(tpp)(acac) complexes, when X-ray diffraction data cannot be obtained. The aim was to determine reliable coordination numbers and interatomic distances, though the very close nature of the scatterers constituting the shell and the water molecules, strong agitation in the crystal, and high thermal motion have increased the difficulties in the fitting procedure. The influence of the acac ligand on the difficulty of fitting the system is acute because its EXAFS signal can extend on no less than four scattering shells, thus increasing the dispersion of distances.

By coupling EXAFS analysis to molecular modeling, we can suggest the octacoordination core geometry of the lanthanide photoabsorber bonded, in the case of Gd(tpp)(acac), to four nitrogen atoms of the tpp porphyrin in a tetradentate fashion to bidentate oxygen atoms of an acetylacetonato anion and to two water molecules. The detection by EXAFS spectroscopy of the second water molecule has proven difficult because of a loose bonding with the metal. Therefore, MM/MD modeling has been used as an additional sensitive means to achieve the determination of the whole coordination geometry for the monomeric Gd complex, suggesting the existence of the two water molecules. Indeed, the existence of the second water molecule is not only supported by the trend of the single-scattering fitting residual but also by the conformation computed by unconstrained molecular dynamics. In turn, we are confident to this molecular dynamics model because it reproduces well the unfiltered EXAFS spectrum, including MS paths and taking into account two water molecules.

For the derivative complexes, our EXAFS analysis showed significant differences either in the change of the rare earth central atom (Gd to Sm) or the porphyrinic ligand (tpp to tpyp). For the Sm(tpp)(acac) complex, an increase of the distances in the first coordination shell related to the increase of the ionic radius has been observed.

The results for the monoporphyrin Gd(tpyp)(acac) are in agreement with a chelating proximal nitrogen from a pyridyl group belonging to a second tetrapyridylporphyrin, associated with a mean distance for the C_α carbon atoms larger than with its tpp analogue. With the bisporphyrin $GdH(tpyp)_2$, we have evidence that the electronic factors such as the degree of extended π-conjugation are strongly correlated to purely structural factors, shedding light on the thermodynamic basicity of porphyrin macrocycle and electrochemical properties. Therefore, the tpyp double decker has much more symmetric distribution of distances and is less sensitive to protonation effects than its analogue with the tpp ligand, as enhanced delocalization of the nitrogen lone pairs leads to a lesser negative charge at the protonation site.

EXAFS investigation on these porphyrinic systems has underlined the interest of associating molecular modeling. The construction of 3D models helps to take into account the multiple scattering paths and yields fit models very close to the experimental observation. From a methodological point of view, it appears worthwhile to continue the effort of developing statistical tests that would help to compare the models and distinguish between accurate models or random fluctuations.

(50) Spyroulias, G. A.; De Montauzon, D.; Maisonat, A.; Poilblanc, R.; Coutsolelos, A. G. *Inorg. Chim. Acta* **1998**, *275*, 182.
(51) Finikova, O. S.; Cheprakov, A. V.; Carroll, P. J.; Dalosto, S.; Vinogradov, S. A. *Inorg. Chem.* **2002**, *41*, 6944.

Acknowledgment. This research was supported by the Greek General Secretariat of Research and Technology and the ΕΠΕΑΕΚ graduate programs of "Bionorganic Chemistry" and "Natural Products" through the Special Research Account of the University of Crete. We would like to also gratefully acknowledge the help of the technical assistance from the LURE laboratory.

Supporting Information Available: Structural data obtained from the best-fit analysis on the raw data of the monomers Sm(tpp)(acac) and Gd(tpyp)(acac) (Table S1) and the dimer GdH(tpyp)$_2$ (Table S2), figure showing the EXAFS of the single- and multiple-scattering paths that produce the largest contribution to the total EXAFS signal (Figure S1). This material is available free of charge via the Internet at http://pubs.acs.org.

IC061861X